Lung Cancer 219 (2026) 109544

Contents lists available at ScienceDirect

Lung Cancer

journal homepage: www.elsevier.com/locate/lungcan

Research Paper

Epiproteomic profiling identifies histone H4 hyperacetylation as a prognostic marker in pleural mesothelioma

Roberta Noberini [a,*], Ioanna Bischinioti [a], Simone Zanetti [a], Alessandro Vai [a], Giulia Sedda [b], Eltjona Mane [c], Claudia Bardoni [d], Giulia Robusti [a], Marianna D'Ercole [c], Rosanna Mancari [e,f], Ugo Cavallaro [a], Nicoletta Colombo [f,g], Luca Bertolaccini [d,h], Mariano Lombardi [c], Nicola Fusco [c,h], Lorenzo Spaggiari [d,h], Domenico Galetta [i], Tiziana Bonaldi [a,h,**]

[a] Department of Experimental Oncology, IEO, European Institute of Oncology IRCSS, 20139, Milan, Italy
[b] Clinical Trial Office, IEO European Institute of Oncology IRCCS, Milan, Italy
[c] Division of Pathology, European Institute of Oncology IRCCS, Milan, Italy
[d] Department of Thoracic Surgery, IEO, European Institute of Oncology IRCCS, Milan, Italy
[e] Gynecologic Oncology Unit, Regina Elena National Cancer Institute, IRCCS, Rome, Italy
[f] Gynecologic Oncology Program, European Institute of Oncology, IRCSS, Milan, Italy
[g] Department of Medicine and Surgery, University of Milano Bicocca, Milan, Italy
[h] Department of Oncology and Hematology-Oncology, University of Milan 20122 Milan, Italy
[i] Division of Thoracic Surgery, Ospedale San Giovanni Bosco, Torino, Italy

ARTICLE INFO

Keywords:
Epigenetics
Epiproteomics
Histone post-translational modification
Histone acetylation
Mass spectrometry
Pleural mesothelioma

ABSTRACT

Pleural mesothelioma (PM) is an aggressive tumor that arises from mesothelial cells as a consequence of asbestos exposure. Despite recent therapeutic advances, the prognosis of PM remains poor, with a median overall survival typically below 18 months.

Here, we investigated the association between alterations in histone post-translational modifications (PTMs) and patient survival in PM by employing state-of-the-art mass spectrometry-based epiproteomics. We profiled a cohort of 96 primary tumors obtained at diagnosis, including a subset of 25 patients with matched pre- and post-neoadjuvant treatment samples. Patients were stratified by overall survival using a 15-month cutoff, which approximates the reported median survival for PM.

Several PTMs in treatment-naïve tumors, as well as a few therapy-induced changes, showed significant differences between short- and long-survivors across the different patient groups. Hyper-acetylation of the histone H4 tail at basal level was significantly and consistently increased in patients with worse prognosis, both in the entire cohort and within individual groups, and was associated with worse overall survival in Kaplan–Meier analyses. This association was independent of established clinicopathological variables in multivariable Cox regression models. Interestingly, increased histone H4 hyperacetylation was observed across multiple tumor types, supporting its broader relevance in cancer biology. In vitro, inhibition of histone acetyltransferases reduced PM cell viability and enhanced sensitivity to cisplatin in a synergistic manner.

These findings identify histone H4 hyperacetylation as an independent prognostic biomarker in PM and highlight epigenetic modulation as a potential therapeutic avenue in PM.

1. Background

Pleural mesothelioma (PM) is a highly aggressive and lethal cancer originating from the mesothelial cells lining the pleura, the membrane surrounding the lungs. It is primarily caused by exposure to asbestos fibers, which induce chronic inflammation and genetic damage over

* Corresponding author.
** Corresponding author at: Department of Experimental Oncology, IEO, European Institute of Oncology IRCSS, 20139, Milan, Italy.
E-mail addresses: roberta.noberini@ieo.it (R. Noberini), tiziana.bonaldi@ieo.it (T. Bonaldi).

https://doi.org/10.1016/j.lungcan.2026.109544
Received 8 May 2026; Received in revised form 14 July 2026; Accepted 17 July 2026
Available online 19 July 2026

several decades. PM is characterized by a poor prognosis, with a 5-year survival rate of approximately 12 % and a median overall survival of less than 18 months after diagnosis [1]. PM comprises three major histological subtypes: epithelioid, sarcomatoid, and biphasic. Epithelioid tumors account for approximately 70–80 % of cases and are generally associated with a more favorable prognosis, while non-epithelioid subtypes display a more aggressive clinical behavior and poorer outcomes [2]. PM treatment is challenging due to its late diagnosis, rapid progression, and resistance to conventional treatments. Therapeutic options include systemic therapies such as chemotherapy, targeted therapy, and radiotherapy, which may be used alone or as part of a multimodal treatment approach. Surgical intervention remains controversial and is generally reserved for patients with early-stage disease who can tolerate invasive procedures. Chemotherapy combining platinum-based agents and pemetrexed has long represented the standard of care for PM. In recent years, the therapeutic landscape of PM has evolved with the introduction of immune checkpoint inhibitors [3]. However, the response to treatment remains heterogeneous and appears to vary according to histological subtype, with the greatest survival advantage observed in patients with non-epithelioid tumors, whereas chemotherapy-based and multimodality strategies continue to represent a major component of the management of epithelioid pleural mesothelioma, particularly in surgically eligible patients [3]. In this context, epigenetic alterations have emerged as potential determinants of tumor behavior and therapeutic vulnerability.

From a molecular perspective, PM is characterized by extensive heterogeneity, encompassing a wide spectrum of genetic and epigenetic alterations that drive tumor initiation and progression. One of the most frequently altered genes in mesothelioma is BRCA1-associated protein 1 (BAP1), a tumor suppressor and epigenetic modifier involved in histone H2A deubiquitination, chromatin remodeling, and transcriptional regulation [4]. BAP1 is a member of the Polycomb Repressive Deubiquitinase (PR-DUB) complex, which catalyzes the deposition of H2AK119Ub and interacts with Polycomb Repressive Complexes (PRC) 1 and 2, with indirect effects on histone H3K27 methylation levels. BAP1 mutations, which occur in 30–65 % of PM cases and are generally associated with loss of protein expression [5], promote the development of cancer across multiple tissue types, with different survival outcomes based on the tumor context. In PM, BAP1 mutations are associated to improved outcomes [6]. Other mutations in epigenetic modifiers include mutations in the histone methyltransferases SETD2, SETDB1, and SETD5, which were found in 2–8 % of cases [7].

Although there is increasing recognition that epigenetic changes play a critical role in PM, the full landscape of these modifications and their clinical implications remains incompletely understood. Traditional methods for studying histone modifications, including immunohistochemistry and Western blotting, are insufficient to detect the full repertoire and combinatorial patterns of histone PTMs. In contrast, mass spectrometry-based proteomics offers a powerful, unbiased, and quantitative approach to quantitatively profile multiple histone PTMs simultaneously in clinical samples. In recent years, we have developed several bottom-up mass spectrometry (MS)–based approaches that enable the profiling of up to 100 differentially modified peptides from both formalin-fixed, paraffin-embedded (FFPE) and frozen patient tissue samples [8–12].

In this study, we employed state-of-the-art MS-based epiproteomics to profile histone acetylations and methylations in PM clinical samples, to investigate the association of epigenetic alterations in histone PTMs with patient survival and treatment response. By analyzing a cohort of 96 primary, treatment-naïve tumors and 25 matched post-therapy samples, we identified epigenetic markers associated with worse survival. In particular, we found that basal-level hyperacetylation of the histone H4 tail was significantly and consistently increased in patients with a worse prognosis, thus representing a potential marker of tumor aggressiveness in PM. In addition, we provide preliminary evidence that pharmacological inhibition of histone H4 acetyltransferases reduces the viability of PM cell lines, supporting the hypothesis that increased histone H4 hyperacetylation may represent both a prognostic marker and a potential therapeutic vulnerability.

2. Materials and methods

2.1. Tissue Specimens

The study was a single-center retrospective study approved by the European Institute of Oncology (IEO) review Board (project code: UID 2395) and was conducted in accordance with the principles stated in the Declaration of Helsinki and good clinical practice. Patient characteristics are reported in Dataset S1. To limit the interference of non-neoplastic tissue, samples pre-treatment were selected to have a tumor cellularity of at least 40 % (range 40–80 %), as routinely adopted for our histone PTM profiling analyses. Post-treatment samples showed a tumor cellularity comprised between 10 and 80 %, reflecting variable residual tumor burden following treatment. High-grade serous epithelial ovarian cancer biopsies were obtained from patients undergoing debulking surgery at IEO Gynaecology Division (protocol R789-IEO). We profiled 38 HGSC FFPE bioptic samples from 28 patients. In some instances, multiple samples from different sites were analyzed from the same patients (Dataset S1). Average values were considered for the analyses

2.2. BAP1 Immunohistochemical staining

Immunohistochemical staining for the BAP1 protein was performed using the labeled streptavidin–biotin (LSAB) staining method. Briefly, 5 μm-thick FFPE sections were mounted onto Superfrost glass slides, deparaffinized and rehydrated. Antigen retrieval was performed in a microwave (750 W) using citrate buffer (pH 6.0) for 10 min, followed by 30 min of cooling. Slides were blocked with Klear dual Enzyme Block (GBI Labs) for 15 min and protein block solution (Dako X0909) for 10 min at room temperature. Sections were incubated with rabbit anti-BAP1 antibody (Invitrogen PA5-105741, 1:150) overnight at 4 °C and 1 h at 37 °C, followed by EnVision Flex + Rabbit Linker (Dako K8019) for 15 min and secondary antibody (Dako EnVision dual link HRP, K4063) for 60 min at room temperature. Immunoreactivity was detected with 3-amino-9-ethylcarbazole (AEC) and counterstained with Mayer's hemalum.

2.3. Sample preparation for MS analysis

Histones were enriched from tissue samples and cell lines as described [10]. About 3 μg of histones per run per sample were mixed with an approximately equal amount of heavy isotope-labelled histones, which were used as an internal standard for quantification to ensure technical reproducibility [13], and were separated on a 17 % SDS-PAGE gel. A band corresponding to the histone octamer was excised, chemically acylated with propionic anhydride, and digested with trypsin. After extraction from the gel, the samples were derivatized with phenyl isocyanate [14]. The samples were desalted on handmade StageTips as previously described [12]

2.4. LC-MS/MS analysis

Histone peptide mixtures were separated by reversed-phase chromatography on an EASY-nLC 1200 high performance liquid chromatography (HPLC) system through an EASY-Spray column (Thermo Fisher Scientific), 25-cm long (inner diameter 75 μm, PepMap C18, 2 μm particles), which was connected online to a Q Exactive plus (Thermo Fisher Scientific) instrument through an EASY-Spray™ Ion Source (Thermo Fisher Scientific). Solvent A was 0.1 % formic acid in ddH_2O, and solvent B was 80 % ACN plus 0.1 % FA. Histone samples were injected in an aqueous 1 % TFA solution at a flow rate of 500 nl/min and were separated with a 50-min linear gradient of 10–45 % solvent B. The Q Exactive

instrument was operated in data-dependent acquisition mode to switch between full-scan MS and MS/MS acquisition automatically. Survey full scan MS spectra (m/z 300–1350) were analyzed in the Orbitrap detector with a resolution of 60,000–70,000 at m/z 200. The 10–12 most intense peptide ions with charge states between 2 and 4 were sequentially isolated to a target MS1 value of 3×10^6 and fragmented by higher-energy collisional dissociation with a normalized collision energy of 28 %. The maximum allowed ion accumulation times were 20 ms for full scans and 80 ms for MS/MS, and the target value for MS/MS was set to 1×10^5. The dynamic exclusion time was set to 10 sec, and the standard mass spectrometric conditions for all experiments were as follows: Spray voltage of 1.8 kV, no sheath and auxiliary gas flow

2.5. MS data analysis

The acquired histone RAW data were analyzed using Epiprofile 2.0 [15], with the SILAC option selected, followed by manual validation [12], which was performed independently of clinical outcome information. For manual analysis, the RAW data were processed using the integrated MaxQuant software v.1.6.2.10, against the Uniprot human proteome (UP000005640), downloaded on 15/02, filtered to retain only histone sequences, and using previously described parameters [12]. Identifications, retention times, and elution patterns were used to guide the manual quantification of each modified peptide using QualBrowser version 2.0.7 (Thermo Fisher Scientific). For each histone-modified peptide, the % relative abundance was estimated by dividing the area under the curve of each modified peptide by the sum of the areas corresponding to all the observed forms of that peptide and multiplying by 100. Light/Heavy (L/H) ratios of %RA were then calculated. L/H ratios for all the samples analyzed are reported in Dataset S2. Given the exploratory nature of this study, candidate histone PTMs were initially identified using nominal p-values. The robustness of significant findings was subsequently assessed using the permutation-based false discovery rate (FDR) procedure implemented in Perseus [16]. FDR correction was applied independently to each differential analysis. The PM mass spectrometry proteomics data have been deposited to the ProteomeXchange Consortium [17] via the PRIDE partner repository with the dataset identifier PXD076262. Data from a previously characterized DIPG cohort, generated as part of a collaborative molecular profiling study conducted within the EPIX-XS consortium, were used to assess H4K5K8K12K16-4ac levels in DIPG samples

2.6. Cell lines and cell culture

IST-MES1 and IST-MES2 (ICLC) cells were grown in Dulbecco modified Eagle medium DMEM, Euroclone Spa) supplemented 10 % Fetal Bovine Serum of North American origin (Euroclone Spa), non-essential amino acids (0.1 mM), and 2 mM L-Glutamine. MSTO-211H cells (DSMZ) were grown in RPMI 1640 (Euroclone Spa) supplemented 10 % Fetal Bovine Serum of North American origin (Euroclone Spa) and 2 mM L-Glutamine. The media were supplemented with penicillin (100 U/ml) and streptomycin (100 mg/ml) (Euroclone Spa). Cells were grown at 37 °C in a 5 % CO2 humidified atmosphere

2.7. Cell treatment and phenotypic assays

MG149 and JG-2016 were purchased from MedChemExpress. IST-MES2 and MSTO-211H cells were treated with DMSO or the compounds for 24 h, in the presence or absence of cisplatin. Cell viability was assessed using the cell Titer Glo (Promega) assay in a 96-well plate after seeding 3000–5000 cells/well. The luminescence was measured with Glomax Explorer. IC50 values were calculated using GraphPad Prism (11.0.0)

2.8. Immunoblot analysis

MSTO211H cells treated with JG-2016 for 24 h were lysed in nuclei isolation buffer supplemented with 0.1 % SDS and 250 U benzonase. 1 μg of proteins was separated on a 4–12 % polyacrylamide pre-cast gel, transferred onto a PVDF (Immobilon, Merck Life Science S.R.L.) membrane and probed by immunoblotting with anti-histone-H4-4ac (1:2000; Millipore, 06–866) and anti-histone H4 antibodies (1:5000; Abcam, ab7311), followed by secondary peroxidase-conjugated antibodies (1:10000; Bio-Rad). Images were acquired on an iBright CL1500 Imaging System and quantified with the iBright analysis Software (v5.6.0, Invitrogen)

2.9. Survival analyses

Survival analyses were performed for the five PTMs showing a significant change in long- vs short survivors by using a FDR cutoff of 0.05 (H3K4me1, H3K9ac|K14ac, H3K27me3K36me2, H4-3ac, H4-4ac). The analysis was performed in R using the survival package, and Kaplan–Meier curves and forest plot were generated with the survminer package (https://www.R-project.org/). Overall survival was defined as the time from the biopsy to death for any cause. Patients who were alive at the last available follow-up were censored on the date of last contact. For each histone PTM, patients were stratified into two groups according to the cohort-specific median value. Differences in survival between groups were assessed using the log-rank test. Adjusted p values were estimated using multivariable Cox proportional hazards regression models including available clinical covariates. Tumor stage was grouped as early (I–II) or advanced (III–IV). Because BAP1 status violated the proportional hazards assumption in a clinical-only model, it was included as a stratification factor in the Cox models. The proportional hazards assumption was tested using Schoenfeld residuals and verified for all variables included in the final model. The interactive web portal UALCAN (https://ualcan.path.uab.edu) was used to analyze the expression levels of histone H4 acetyltransferases in PM, leveraging data from The cancer Genome Atlas (TCGA) database

3. Results

3.1. Mass spectrometry-based profiling in treatment-naïve PM clinical samples

We analyzed a cohort of 96 primary, treatment-naïve epitheliod PMs tumors collected between 1998 and 2021 (Fig. 1A and Dataset S1), which included 71 patients who did not receive surgery and 25 patients who underwent surgery following neoadjuvant therapy. For the latter group, paired pre- and post-therapy samples were analyzed to assess whether therapy-induced epigenetic changes correlate with treatment response and survival. The samples were categorized as “short-term survivors” with survival less than 15 months, or “long-term survivors” with survival greater than 15 months. This cutoff was selected because it approximates the median overall survival reported in large clinical series of PM, thereby enabling the identification of biologically meaningful prognostic groups.

We employed a state-of-the-art quantitative MS workflow to profile histone acetylations and methylations in PM clinical samples (Fig. 1B). Histones were extracted from FFPE tissues using the PAT-H-MS protocol [12] and were digested with an in-gel digestion protocol involving the double derivatization of lysines and peptide N-termini, which has been shown to improve the detection of short and hydrophilic peptides and to enable the analysis of the highest number of modified peptides in a single run [14]. Heavy-isotope-labeled histones were added to each sample as a spike-in internal standard before digestion, to enhance technical reproducibility and quantitation accuracy [13].

The heatmap in Fig. 1C summarizes the results from our epiproteomics profiling. We quantified up to 38 differentially modified

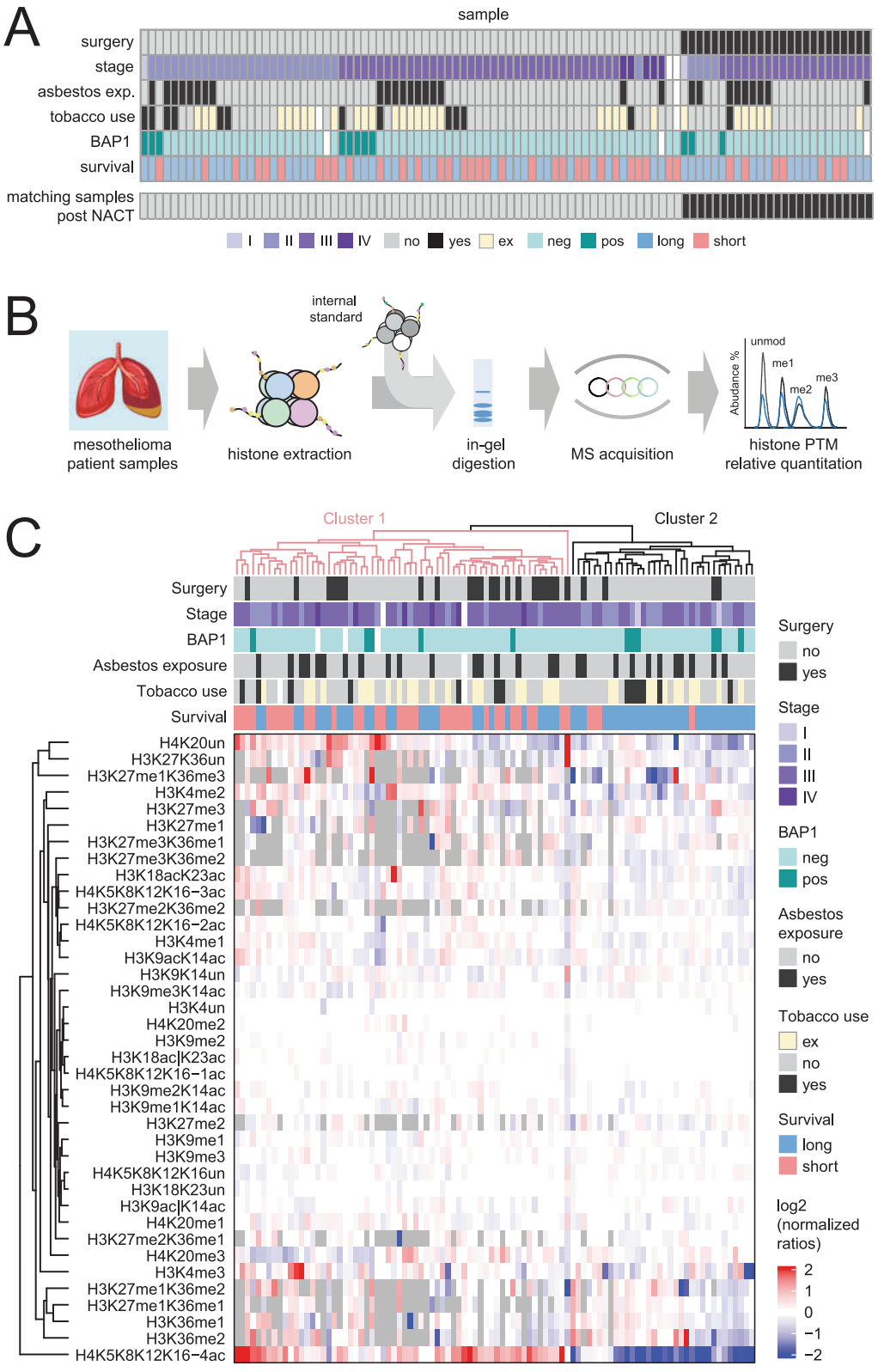

Fig. 1. Mass spectrometry-based histone PTM profiling of mesothelioma patient samples. (A) Mesothelioma cohort overview. Survival is defined based on a 15-months cutoff. White: unknown. (B) Schematic description of the MS-based experiment, which includes histone extraction from FFPE sections from mesothelioma samples, mixing with an internal standard, SDS-PAGE separation, in-gel histone digestion, and liquid chromatography- mass spectrometry (LC–MS) acquisition and quantification of histone PTM levels. Image by brgfx on FreePix. (C) Hierarchical clustering based on log2(L/H ratios) obtained for histone PTMs in mesothelioma samples. L/H (light/heavy) relative abundance ratios were obtained using a spike-in strategy (light channel: sample, heavy channel: spike-in standard), and were normalized to the average ratios across samples. The grey color in the heatmap indicates peptides that were not quantified. Euclidean distance and complete linkage were employed for both row and column clustering.

peptides from archival FFPE PM tissues, excluding modifications previously shown to be affected by FFPE storage, such as H3K79 and H3K18 methylations [12]. Hierarchical clustering based on histone PTM levels generated two main clusters characterized by distinct histone PTM profiles, most notably by different levels of the tetra-acetylated form of the histone H4 tail (peptide H4K5K8K12K16-4ac), which contains four acetylated lysines and corresponds to hyper-acetylated histone H4. Notably, cluster #1, which was characterized by higher H4K5K8K12K16-4ac levels, contained 27 long-survivors and 35 short-survivors. In contrast, cluster #2, which comprised samples with lower H4K5K8K12K16-4ac levels, contained 30 long-survivors and 4 short-survivors, resulting in a highly significant association between clustering based on histone PTM profiles and survival (p = 2.3e-05 by Fisher's exact test).

3.2. Correlation between histone PTMs and clinical features

To assess whether histone PTM–based sample profiles reflected known clinical or molecular determinants of PM outcome, we evaluated the impact of established prognostic variables and other clinical features on the epigenetic profiles of the PM cohort. Patients were stratified according to disease stage and BAP1 mutational status, as well as clinical

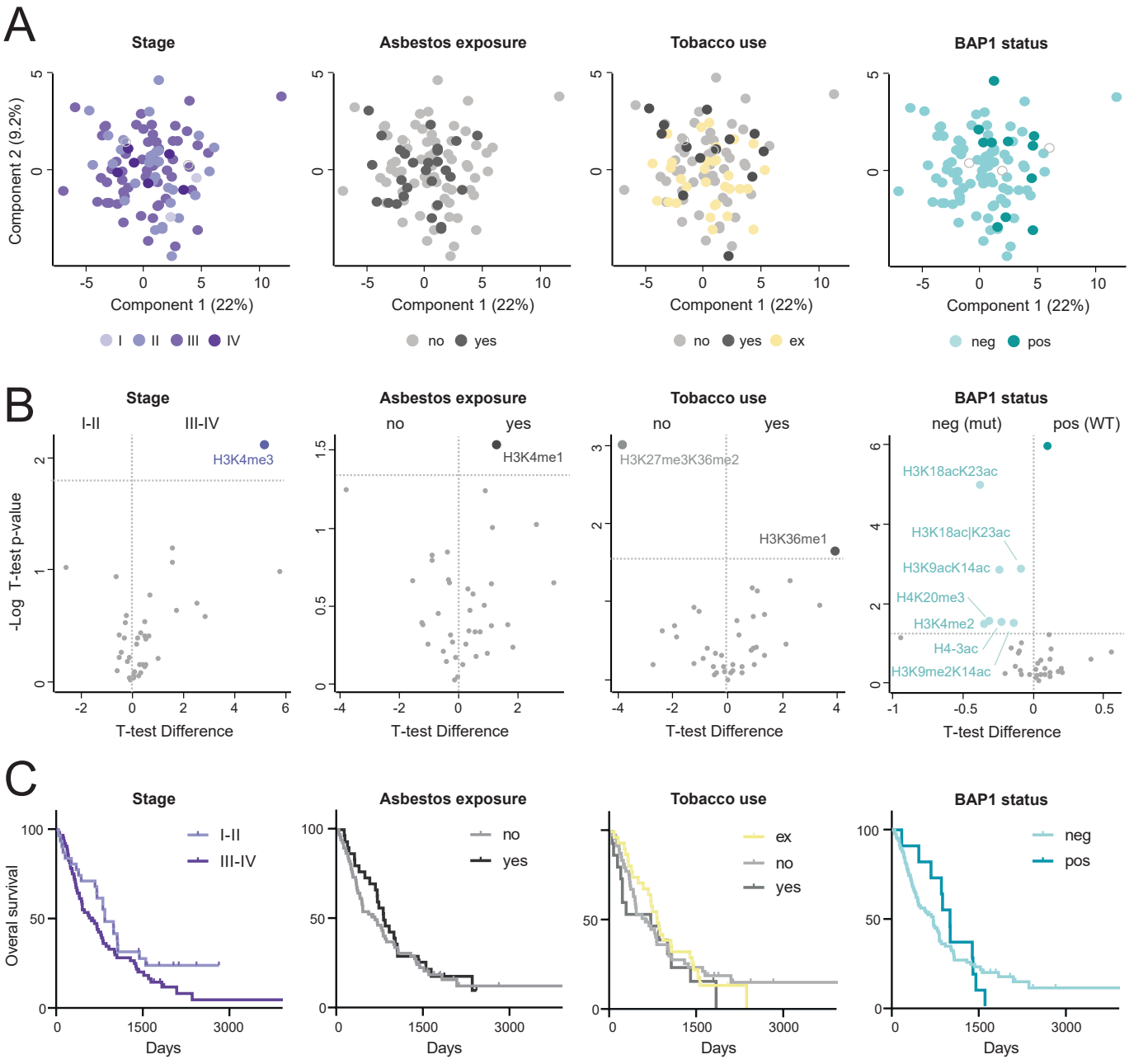

Fig. 2. Histone PTM profiles and clinical features in mesothelioma. (A) PCA based on histone PTM data obtained from the profiling of PM samples. Different colors refer to different tumor stages, asbestos exposure, tobacco use, or BAP mutational status. Empty circle: no information available. (B) Volcano plot showing significantly regulated histone PTMs in stages III-IV vs I-II, and in tumors from patients with different asbestos exposure, tobacco use, and BAP1 status. The horizontal line represents the threshold of statistical significance ($p < 0.05$ by two-tailed Welch's *t*-test). The symbol "|" indicates that the modification is present on only one of the indicated residues. Unmodified peptides are not labelled. (C) Kaplan-Meier curve displaying the estimated overall survival (OS) probability for groups of mesothelioma samples defined based on tumor stages, asbestos exposure, tobacco use, or BAP mutational status. No significant differences were observed among curves by the log-rank test. Pos = positive IHC staining for BAP1 (BAP1 WT); neg = negative IHC staining for BAP1 (BAP1 mutations).

features including asbestos exposure and tobacco use. Principal component analysis (PCA) did not reveal clustering of samples based on any of these variables, indicating that global histone PTM patterns are independent of them (Fig. 2A). However, a few histone PTMs were associated with specific clinical or molecular features (Fig. 2B). In particular, H3K4me3 was increased at higher stages, H3K4me1 in tumors from patients with asbestos exposure, and H3K36me1 and H3K27me3K36me2 were significantly different in patients with different tobacco exposure. Because inactivating BAP1 mutations are found in a high proportion of PMs and can have secondary effects on various histone PTMs, we also examined correlations between histone PTM levels and BAP1 status. Loss of BAP1 protein, which is indicative of inactivating mutations, was evaluated in tumor samples by immunohistochemistry (IHC). Several acetylation marks were decreased in BAP1 mutant tumors, as well as H3K4me2 and K4K20me3.

In addition, Kaplan–Meier analyses (Fig. 2C) showed no significant differences in overall survival in our cohort when patients were stratified by stage, asbestos exposure, tobacco use, or BAP1 status. This lack of association may reflect cohort-specific factors, including limited sample size for certain subgroups and heterogeneity in treatment regimens, highlighting that conventional clinicopathological factors do not fully capture the variation in patient outcomes in this dataset.

3.3. Increased H4K5K8K12K16-4ac associates with worse survival in PMs

To investigate whether histone PTM levels can stratify PM patients by survival, we compared short- and long-term survivors. When analyzing the whole cohort of samples regardless of treatment, short-term survivors showed significantly higher levels of H4K5K8K12K16-3ac and H4K5K8K12K16-4ac (labelled H4-3ac and H4-4ac in Fig. 3A), two markers of histone H4 hyperacetylation. Other significant changes included increases in H3K4me1/me3, and H3K27me3K36me2, and a decrease in H3K9|K14ac in short-term vs long-term survivors. We also analyzed the epigenetic profiles of patients stratified by treatment type ("no surgery" and "surgery"). The most marked and reproducible alteration in short survivors was again an increase in H4K5K8K12K16-4ac, which showed a significant and close-to-significant increase in short-survivors in the surgical and non-surgical cohort, respectively. In addition, this mark remained significant after permutation-based false discovery rate (FDR) correction in the whole cohort and in the non-surgical cohort (Fig. 3A-B). To assess the robustness of these findings, we repeated the differential PTM analysis using the cohort-specific median overall survival (23.3 months) as an alternative cutoff. This sensitivity analysis further demonstrated the robustness of our findings and confirmed H4K5K8K12K16-4ac as the histone PTM most consistently associated with poor survival (Fig. S1). In agreement with these results, H4K5K8K12K16-4ac was the main contributor to the partial separation of samples with different survival by PCA, as indicated by the greater magnitude of its loading vector in the PCA biplot. H4K5K8K12K16-3ac was also among the top 10 contributors, although with a lower weight.

To avoid potential biases due to the cutoffs used to define long- and short-term survivors, we also investigated the association between histone PTMs and overall survival probability using Kaplan-Meier analyses. Patients with higher H4K5K8K12K16-4ac levels showed a trend toward worse overall survival in the whole cohort (log-rank $p = 0.076$) and a significant difference in the non-surgical cohort (Fig. 3D). Baseline clinicopathological characteristics according to H4K5K8K12K16-4ac status are summarized in Table S1. Patients with high H4K5K8K12K16-4ac levels were more frequently represented in the surgical cohort, whereas no significant differences were observed for asbestos exposure, smoking status, or disease stage.

To further evaluate the effect of H4K5K8K12K16-4ac relative to other clinical and exposure-related variables, we performed a multivariable Cox regression analysis including treatment type, age, sex, asbestos exposure, smoking status, and disease stage. Performance status data were not available for a sufficiently large proportion of patients to allow robust statistical modeling, which represents a limitation of this analysis. H4K5K8K12K16-4ac remained significantly associated with overall survival and showed the largest effect size among all variables included in the model (Fig. 3E). In addition, treatment group, sex, and disease stage were significantly associated with survival. These findings suggest that this epigenetic mark may capture biologically relevant features of tumor aggressiveness that are not fully reflected by traditional clinicopathological parameters. Taken together, these findings support the prognostic relevance of H4K5K8K12K16-4ac in PM. Importantly, this association was observed across different treatment groups, suggesting that histone H4 hyperacetylation reflects intrinsic tumor biology rather than treatment-related effects. Among the additional PTMs remaining significant after FDR correction, H3K4me1 also showed a consistent association with poor outcome in both Kaplan–Meier and multivariable Cox analyses (Fig. S2), suggesting that it may represent an additional epigenetic feature associated with poor prognosis in PM.

Remarkably, histone H4 hyperacetylation appears to be associated with tumor development and aggressiveness not only in PM, but also in other tumors. Indeed, H4K5K8K12K16-3ac or H4K5K8K12K16-4ac were upregulated in breast cancer (data from [18]), uveal melanoma (data from [19]), and diffuse intrinsic pontine glioma (DIPG) compared with normal tissues (Dataset S2)(Fig. S3A). In addition, higher levels of H4K5K8K12K16-3ac were associated with worse overall survival in a cohort of high-grade serous ovarian carcinoma (HGSOC) (Fig. S3B). These results indicate that histone H4 hyperacetylation is associated with tumor progression and poor clinical outcomes across diverse cancer types.

3.4. Neoadjuvant chemotherapy induces histone PTM changes associated with patient survival

We next asked which histone PTM changes are induced by neoadjuvant chemotherapy, and whether they are also associated with patient survival in PM. The comparison of the epigenetic profiles of paired pre- and post-neoadjuvant therapy samples from 25 patients identified several significant therapy-induced changes, including a marked increase in acetylation of histones H3 and H4 and a decrease in H3K9me2 (Fig. 4A and S4A-B). However, histone PTM levels are known to vary with cell-cycle progression and proliferative activity and the modifications identified here have previously been shown to change in the opposite direction in proliferative G2/M−phase cells in a breast cancer cell line model (Fig. S4C)[18], suggesting that the increased histone acetylation and the reduction in H3K9me2 observed after therapy may, at least partially, reflect a shift toward a less proliferative tumor cell state following chemotherapy rather than a direct, therapy-specific epigenetic effect [18]. In addition, one limitation of this analysis is that the tumor cellularity after treatment was rather variable, ranging from 10 to 80 %.

To determine whether these therapy-associated changes were associated with clinical outcome, we stratified patients by survival. The increase in acetylation marks in post-therapy samples was maintained when long- and short-survivors were analyzed separately, consistent with this effect being a general consequence of treatment-induced changes in proliferation rather than a survival-specific epigenetic signature. In contrast, few histone marks showed survival-associated patterns (Fig. S4D-E). The most interesting was a decrease of H3K9me3K14ac following therapy, uniquely observed in long-survivors (Fig. 4B, Fig. S4D). Accordingly, the post/pre treatment ratio for these two marks was significantly different between long- and short-survivors (Fig. 4C, Fig. S4E).

These findings indicate that specific histone PTM changes may be associated with differential clinical outcomes following neoadjuvant chemotherapy.

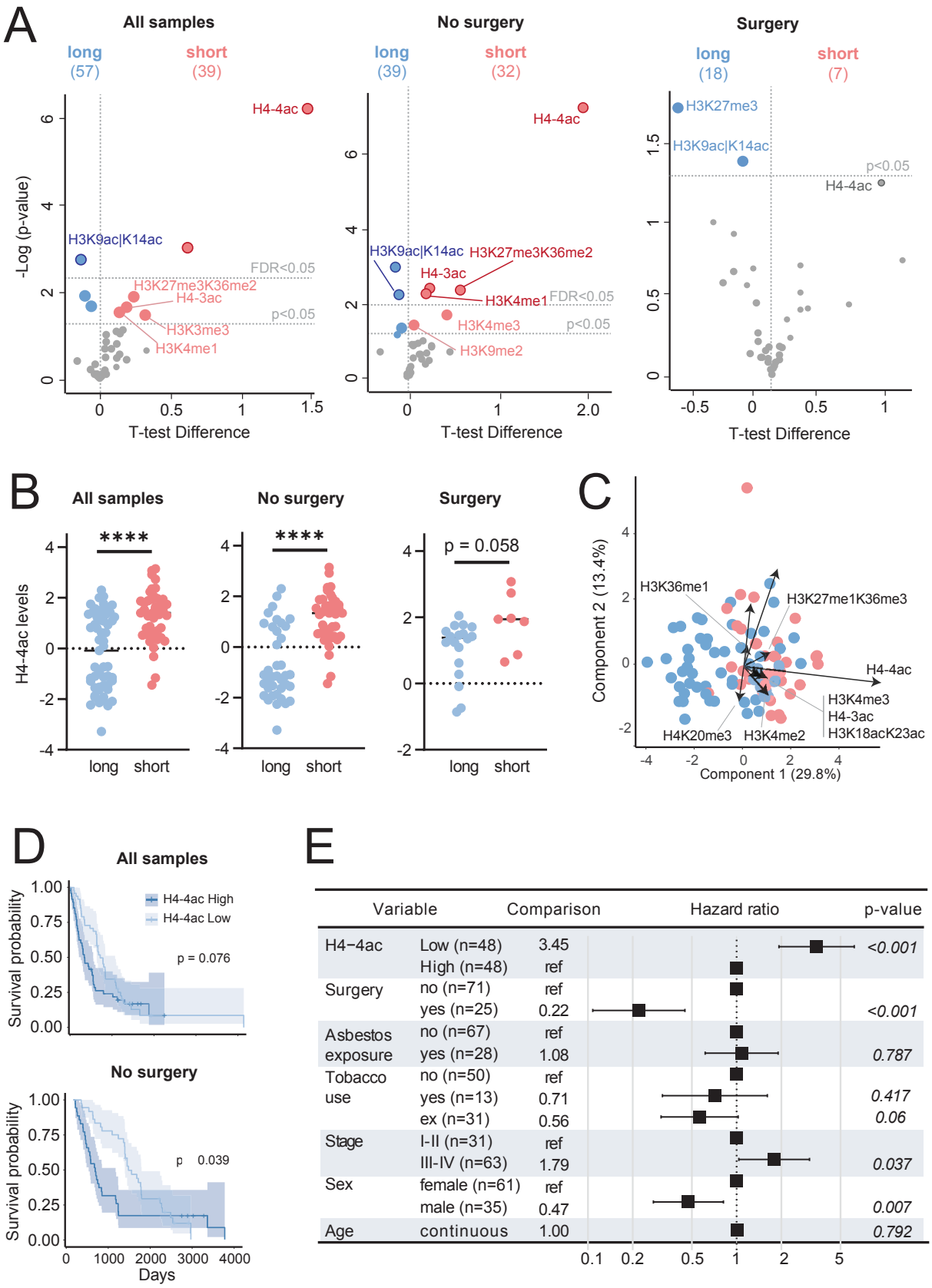

(caption on next page)

Fig. 3. Histone H4 hyperacetylation is associated with worse prognosis in PM. (A) Volcano plots showing histone PTM changes versus *P* values in PM stratified by overall survival (>15 months: long-survivors, <15 months: short-survivors) in all the samples analyzed (left panel), in patients that did not undergo surgery (middle panel), and in patients that underwent surgery (right panel). The horizontal lines represent the threshold of statistical significance (bottom line: $p < 0.05$, top line: false discovery rate (FDR) < 0.05 by two-tailed Welch's *t*-test). Unmodified peptides are not labelled. Symbols with darker outlines represent significant changes based on FDR, which accounts for multiple comparisons. The symbol "|" indicates that the modification is present on only one of the indicated residues. (B) Log2(L/H ratios) for H4K5K8K12K16-4ac in the indicated patient cohorts. * $p < 0.05$; ****$p < 0.0001$ by two-tailed Welch's *t*-test. Horizontal bar: mean. (C) Principal component analysis (PCA) based on histone PTM profiles obtained from the samples shown in A. Patients with at least 70 % valid values are shown. Missing values were replaced with 0 after z-score transformation. (D) Kaplan-Meier curves showing the estimated overall survival (OS) probability for two groups of PMs defined by the level of H4K5K8K12K16-4ac in the whole cohort (top panel) and in patients that did not undergo surgery (bottom panel). The p-value from a log-rank test is indicated. Shaded areas depict the 95 % confidence interval. (E) Forest plot showing hazard ratios for H4K5K8K12K16-4ac (H4-ac) and various clinical and molecular variables, including tumor stages, asbestos exposure, and tobacco use. P values were derived from multivariable Cox regression analysis.

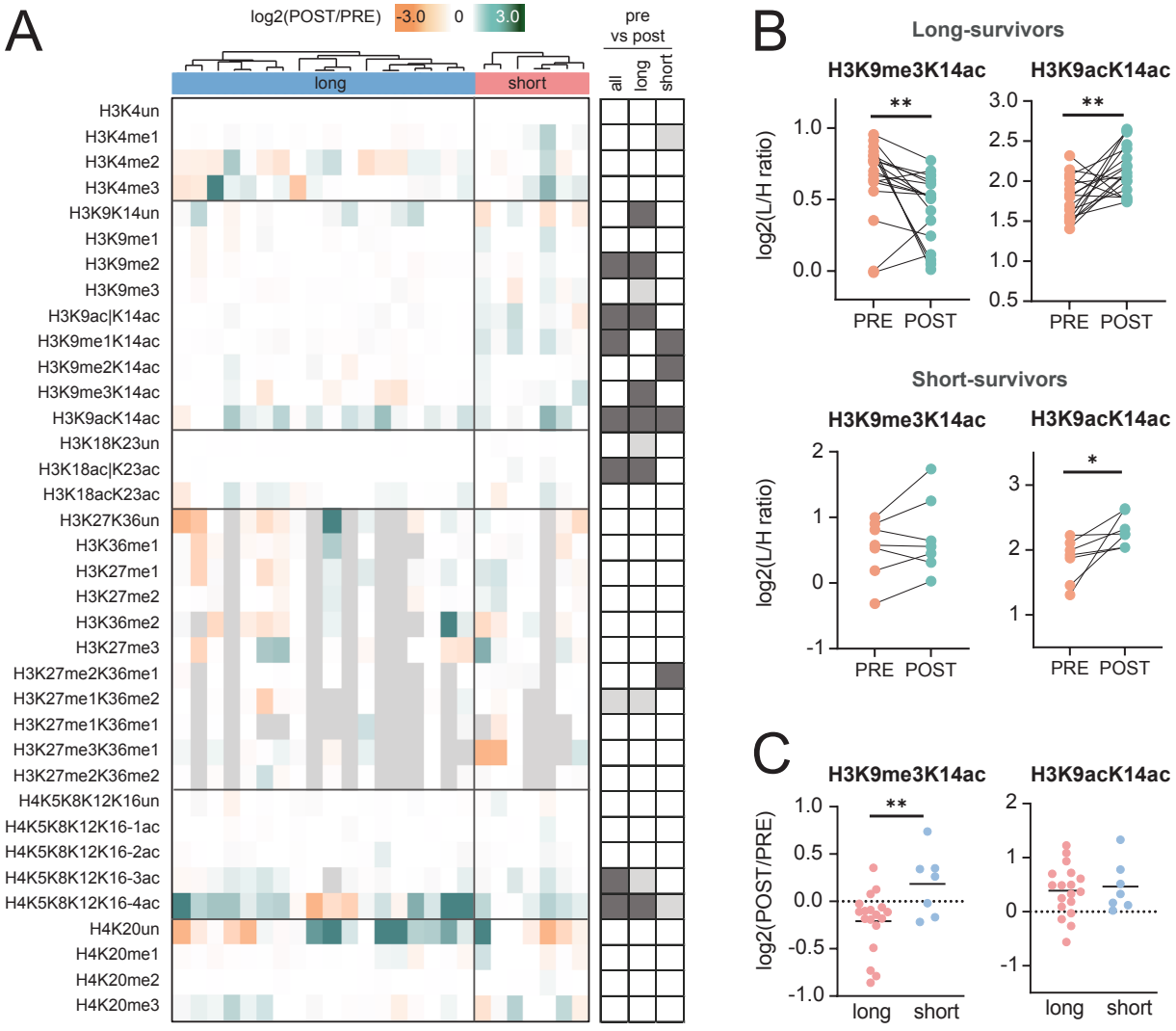

Fig. 4. Analysis of histone PTM changes induced by neoadjuvant chemotherapy and associated with patient survival. (A) Heatmap display of the log2 ratios of histone PTM levels post/pre-chemotherapy. The grey color indicates peptides that were not quantified. The right panel highlights significant changes ($p < 0.05$ by two-tailed paired Student's *t* test, dark grey) or a close-to-significant change ($0.05 < p < 0.1$, light grey) for the comparison of pre- and post-chemotherapy samples in the whole patient cohort, in long-survivors, and in short-survivors. (B) Log2(L/H ratios) for the indicated histone PTMs in matched PM samples pre-/post-adjuvant chemotherapy. * $p < 0.05$; **$p < 0.01$ by two-tailed paired Student's *t*-test. (C) Histone PTM ratios between post and pre-chemotherapy samples in long and short survivors. * $p < 0.05$; **$p < 0.01$ by two-tailed Student's *t*-test.

3.5. Inhibition of histone acetyltransferases reduces mesothelioma cell growth in vitro

Our results showed that histone H4 hyperacetylation is associated with worse overall survival in PMs. We therefore hypothesized that decreasing histone H4 hyperacetylation may represent a therapeutic avenue for treating PMs. KAT5 (also known as Tip60), an acetyltransferase that modifies H3K14 and histone H4 lysines, has been reported to be upregulated in PM compared to benign pleura [20]. In addition, we found that increased transcript levels of HAT1, an histone H4 acetyltransferase, are observed in multiple tumor types compared to normal tissues (https://www.proteinatlas.org/ENSG00000128708-HAT1/cancer) and are significantly associated with worse survival in a cohort of PMs from the TCGA database (Fig. 5A). To identify the most

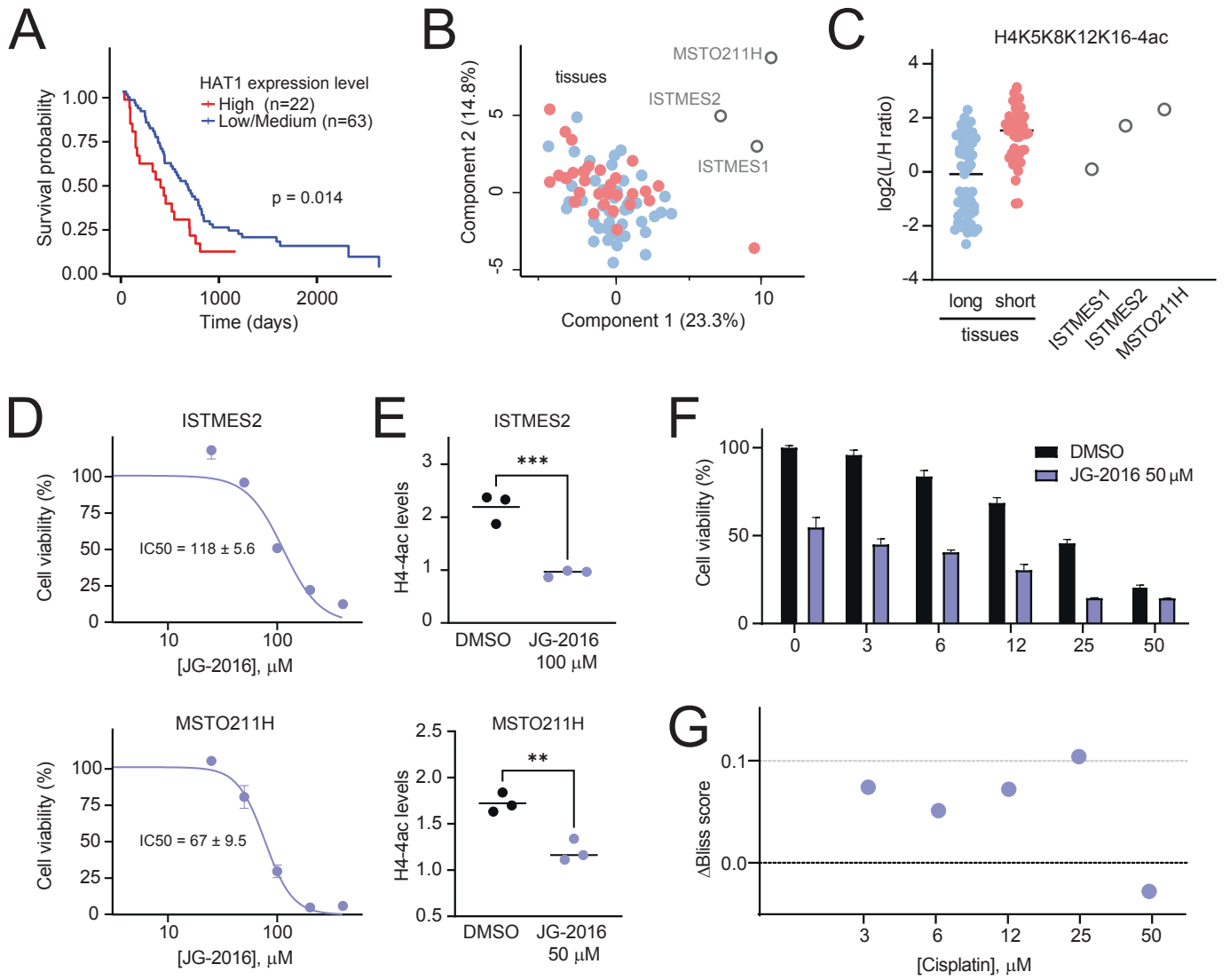

Fig. 5. Inhibiting histone H4 acetyltransferases reduces PM cell growth in vitro. (A) Kaplan-Meier curve displaying the estimated overall survival (OS) probability for groups of mesothelioma samples defined based HAT1 expression levels obtained from the UALCAN portal [24]. (B) Principal component analysis (PCA) based on histone PTM data obtained from PM patient tissues and cell lines. Red: short survivors, blue: long survivors. Patients with at least 70 % valid values are shown. Missing values were replaced with 0 after z-score transformation. (C) H4K5K8K12K16-4ac levels (expressed as L/H ratios, where L: sample and H: internal standard) in PM patient tissues and cell lines. Horizontal bar: mean. (D) Viability dose–response curve for ISTMES2 and MSTO211H cells treated with increasing concentrations of JG-2016 for 24 h. Error bars=SEM from three technical replicates. IC50 value are reported as average ± SEM from 2 biological replicates. (E) Percentage of viable MSTO211H cells after treatment with JG-2016 in combination with cisplatin for 24 h. The data were normalized to the untreated condition. Error bars=SEM from three technical replicates. (F) ΔBliss values were plotted as a function of cisplatin concentration. Values were calculated as ΔBliss = E_observed − E_expected using the Bliss independence model (E = 1 − viability/100). Each point represents the mean of replicates; the horizontal line indicates ΔBliss = 0 as a reference for additive effects. (For interpretation of the references to colour in this figure legend, the reader is referred to the web version of this article.)

suitable cellular model to test histone H4 acetyltransferase inhibitors, we profiled histone PTMs in three PM cellular models: ISTMES1, ISTMES2, and MSTO-211H. All cell lines showed a distinct epigenetic profile compared with the epigenetic profiles of PM tissue, with changes in multiple sites (Fig. S5) that were previously reported in other culture models [21]. Among the cell lines tested, ISTMES2 showed the profile closest to the tissues (Fig. 5B). When focusing on histone H4 hyper-acetylation, we found high levels of H4K5K8K12K16-4ac in ISTMES2 and MSTO-211H cells, resembling those observed in short-survivor patients (Fig. 5C). We therefore tested the KAT5 inhibitor MG-149 [22] and the HAT1 inhibitor JG-2016 [23] in these two cell line models.

MG-149 treatment for 24 h reduced ISTMES2 and MSTO-211H cell viability with IC50 values of 155 and 110 μM, respectively (Fig. S6A). However, quantitative MS showed only a modest reduction in H4K5K8K12K16-4ac levels at concentrations close to the respective IC50 values (Fig. S6B), and the compound displayed predominantly additive interactions when combined with cisplatin (Fig. S6C-D). In contrast, JG-2016 showed higher antiproliferative activity (IC50 67–118 μM; Fig. 5D) and significantly reduced H4K5K8K12K16-4ac levels in both cell lines, confirming direct target engagement, as measured by MS (Fig. 5E) and immunoblot analyses (Fig. S7A). Global histone PTM profiling also showed a decrease in other multiply acetylated forms of histone H4, including H4K5K8K12K16-3ac, which was also associated with poor prognosis in our patient cohort. In addition, treatment with JG-2016 decreased several acetylation marks on histone H3, consistent with previous observations that perturbation of HAT1 activity can indirectly impair H3 acetylation during chromatin assembly [25] (Fig. S7B). Finally, positive Bliss scores were observed for JG-2016 at low to intermediate cisplatin concentrations (3–25 μM), indicating greater-than-additive effects.

These results suggest targeting histone H4 acetylation as a potential therapeutic avenue to treat PM, with HAT1 inhibition as the most promising therapeutic strategy among those evaluated in this study. Although these findings are preliminary and derived from in vitro models, they provide a rationale for further investigation of HAT1 inhibition in mesothelioma, particularly in tumors with high basal levels of histone H4 acetylation.

4. Discussion

In this study, we provide the most comprehensive quantitative analysis to date of histone post-translational modifications in primary PM samples, identifying epigenetic patterns associated with patient survival and response to therapy.

We observed limited associations between histone PTM patterns and smoking history, asbestos exposure, or tumor stage, suggesting that the tumor epigenetic landscape is largely independent of classical environmental and clinical risk factors, at least in our cohort. While asbestos exposure is the dominant etiologic factor for PM and has been linked to changes in DNA methylation in lung cancer [26], there is limited evidence directly connecting specific histone PTM patterns to exposure history or clinical stage in human tumors. We previously reported that BAP1 mutations are associated with several changes in histone PTMs in uveal melanoma [19]. Interestingly, the changes observed in PM BAP1-mutated tumors are generally opposite to those we observed in uveal melanoma. Clinically, BAP1 mutations correlate with a better prognosis in PM [6] but are associated with worse outcomes in uveal melanoma [27], reflecting tissue-specific roles of BAP1 in chromatin regulation and disease outcomes that may explain this result.

The most notable finding from our profiling is the association of basal histone H4 hyperacetylation with poorer prognosis in PM. This association emerged from differential analyses of samples stratified by survival using a 15-months cutoff and was confirmed in a sensitivity analysis using the cohort-specific median overall survival, as well as in multivariable Cox regression analyses. From a clinical perspective, identifying a reproducible epigenetic marker associated with survival is particularly relevant in PM, a disease in which prognostic stratification remains largely based on clinical stage and performance status. This epigenetic alteration does not appear to be a consequence of higher tumor cell proliferation in more aggressive tumors, as dividing cells generally show decreased histone acetylation [18]. These findings highlight H4 hyperacetylation as a potential prognostic biomarker in PM, which could help identify patients with more aggressive disease and support the investigation of epigenetic therapeutic strategies in PM. Remarkably, this mark was also increased in different tumor types compared with normal tissues, and a similar association between histone H4 hyperacetylation and poor prognosis was observed in ovarian cancer, suggesting that this change may represent a conserved epigenetic state associated with aggressive tumor biology across cancer types. One possible explanation is that widespread histone hyperacetylation may contribute to a more permissive chromatin state that supports oncogenic transcriptional programs, a mechanism consistent with the global DNA hypomethylation commonly observed in cancer [28], which also promotes chromatin accessibility and transcriptional deregulation.

H3K4me1 also emerged as a reproducible survival-associated PTM. In addition to being increased in short survivors, higher H3K4me1 levels were associated with poorer overall survival in both Kaplan–Meier and multivariable Cox analyses. This mark is typically associated with active enhancer regions and has been reported to play a dual role in cancer [29]. Notably, H3K4me1-marked enhancers were enriched at resistance-driving genes in therapy-resistant prostate cancers [30], highlighting a potential link between H3K4me1 and a more aggressive tumor phenotype.

Additional therapy-associated epigenetic alterations were identified by comparing histone PTM levels pre- and post-neoadjuvant chemotherapy. Neoadjuvant treatment induced widespread changes in histone acetylation, including increased H4K5K8K12K16-4ac, which likely reflect, at least in part, the reduced proliferative activity induced by chemotherapy, as supported by the opposite regulation of these PTMs during cell-cycle progression in proliferating cancer cells (Fig. S4C). The chemotherapy-induced increase in histone acetylation and the association between basal H4 hyperacetylation and poor survival therefore likely reflect distinct biological processes. Instead, the decrease in H3K9me3K14ac following therapy observed exclusively in long survivors may reflect biological processes associated with favorable clinical outcome. Co-occurrence of the repressive mark H3K9me3 and the activating mark H3K14ac has been shown to define a form of bivalent chromatin characterized by an inactive, “poised” state [31]. This combination of modifications is recognized by the SETDB1 methyltransferase and is involved in the silencing of endogenous retroviral elements [32]. H3K14ac has been reported to facilitate recruitment of SETDB1 to these loci, promoting deposition of H3K9me3 and suppression of tumor-intrinsic immunogenicity [33]. This result raises the possibility that pharmacological modulation of SETDB1 could represent a strategy to enhance tumor immunogenicity and treatment response in PM. It must be noted that −given the variable residual tumor cellularity of post-treatment specimens- the contribution of stromal and inflammatory components to these changes cannot be excluded. Future studies incorporating systematic tumor purity assessment or spatially resolved approaches will be important to further define the cellular origin of the observed epigenetic alterations.

Beyond its prognostic value, histone H4 hyperacetylation may represent a potential target for PM treatment. Our functional studies provide preliminary support for this hypothesis, showing that pharmacological inhibition of HAT1 reduces H4K5K8K12K16-4ac and cell viability in cell line models. Previous preclinical studies have focused on histone deacetylases (HDACs) as potential targets, reporting that HDAC inhibitors can induce apoptosis, cell-cycle arrest, and enhance chemotherapy sensitivity in mesothelioma cell lines, particularly in the context of BAP1 loss, which alters HDAC1/2 activity and chromatin regulation [34]. However, clinical trials of single-agent HDAC inhibitors failed to improve survival in unselected patients [35]. Our results show that tumors with high H4 acetylation are associated with shorter survival and somewhat contradict these previous findings. One hypothesis is that aggressive PMs may already be in a hyper-acetylated state and thus less dependent on HDAC activity, potentially explaining the limited clinical efficacy of HDAC inhibition in PM. Conversely, pharmacologic inhibition of acetyltransferases may represent a more effective strategy, particularly in aggressive and chemoresistant tumors, warranting further investigation.

The interpretation of our findings should be considered in the context of the evolving therapeutic landscape of PM. Recent clinical trials have established immune checkpoint inhibitors as an important treatment option for PM, although treatment benefit appears to vary substantially according to histological subtype, with the most pronounced survival advantage reported in non-epithelioid tumors [3]. Notably, all tumors included in our cohort were of epithelioid histology, the most common subtype of pleural mesothelioma. Although current treatment paradigms increasingly incorporate immunotherapy, chemotherapy-based and multimodality strategies remain integral components of the therapeutic management of epithelioid disease. Therefore, we believe that the prognostic and therapy-associated epigenetic alterations identified in this study remain clinically relevant. Nevertheless, future studies will be required to determine whether these biomarkers retain their prognostic value in contemporary cohorts receiving immunotherapy-based treatments. Furthermore, our findings derive from a retrospective single-center cohort and should therefore be prospectively validated in independent multicenter series, particularly in patients treated with contemporary chemo-immunotherapy regimens.

Altogether, these findings suggest histone H4 hyperacetylation as a potential prognostic biomarker in PM and indicate that therapeutic strategies aimed at modulating histone acetylation should be explored in

a more biologically stratified patient population.

Funding sources

- Fondazione Buzzi Unicem ETS.
- Italian Association for Cancer Research (AIRC), grant number and IG-2023–28767 (TB).
- Italian Ministry of Health with "Ricerca Corrente 5x1000".
- The analysis of DIPG samples Supported by EPIC-XS, project number 823839, funded by the Horizon 2020 programme of the European Union

CRediT authorship contribution statement

Roberta Noberini: Writing – original draft, Validation, Methodology, Formal analysis, Conceptualization. **Ioanna Bischinioti:** Methodology, Investigation. **Simone Zanetti:** Investigation. **Alessandro Vai:** Visualization, Formal analysis. **Giulia Sedda:** Resources. **Mane Eltjona:** Resources. **Bardoni Claudia:** Resources. **Giulia Robusti:** Investigation. **Marianna D'Ercole:** Investigation. **Rosanna Mancari:** Resources. **Ugo Cavallaro:** Resources. **Nicoletta Colombo:** Resources. **Luca Bertolaccini:** Resources. **Mariano Lombardi:** Resources, Investigation. **Nicola Fusco:** Resources. **Lorenzo Spaggiari:** Supervision, Funding acquisition. **Domenico Galetta:** Conceptualization. **Tiziana Bonaldi:** Writing – review & editing, Supervision, Funding acquisition, Conceptualization.

Declaration of competing interest

The authors declare the following financial interests/personal relationships which may be considered as potential competing interests: [Tiziana Bonaldi reports financial support was provided by Fondazione Buzzi Unicem. Tiziana Bonaldi reports financial support was provided by AIRC Foundation for Cancer Research. Lorenzo Spaggiari reports financial support was provided by Italian Ministry of health. Tiziana Bonaldi reports financial support was provided by Horizon 2020 programme of the European Union. If there are other authors, they declare that they have no known competing financial interests or personal relationships that could have appeared to influence the work reported in this paper.].

Acknowledgements

We thank Betül Çat, Chiara Ghirardi and Sigrid Verhelst for technical help, and Clarissa Uslenghi for helping with the retrieval of clinical data. We also thank Amit Sharma, Jaroslaw Maciaczyk, and Javad Nazarian for providing access to the DIPG dataset. Ioanna Bischinioti and Alessandro Vai are PhD students within the European School of Molecular Medicine (SEMM). Alessandro Vai was supported by an AIRC fellowship for Italy. The authors used ChatGPT Enterprise (OpenAI) for proofreading. All outputs were critically reviewed and edited by the authors, who take full responsibility for the content of this manuscript. The authors gratefully acknowledge the financial support of Fondazione Buzzi Unicem ETS for supporting this project and for covering the publication costs.

Ethics approval and consent to participate.

PM and high-grade serous epithelial ovarian cancer samples were obtained from patients undergoing surgery at the European Institute of Oncology (Milan). The patients provided informed consent and this study was approved by the Ethical Committee of the European Institute of Oncology (Study UID 2395 and R789-IEO).

Availability of data and materials.

The PM MS proteomics data have been deposited to the ProteomeXchange Consortium via the PRIDE partner repository with the dataset identifier PXD076262**.** The other datasets supporting the conclusions of this article are included as additional files.

Appendix A. Supplementary data

Supplementary data to this article can be found online at https://doi.org/10.1016/j.lungcan.2026.109544.

References

[1] B. Bertin, M. Zugman, G. Schvartsman, The current treatment landscape of malignant pleural mesothelioma and future directions, cancers (Basel) 15(24) (2023).

[2] R.R. Meyerhoff, C.F. Yang, P.J. Speicher, B.C. Gulack, M.G. Hartwig, T.A. D'Amico, D.H. Harpole, M.F. Berry, Impact of mesothelioma histologic subtype on outcomes in the surveillance, epidemiology, and end results database, J. Surg. Res. 196 (1) (2015) 23–32.

[3] P. Baas, A. Scherpereel, A.K. Nowak, N. Fujimoto, S. Peters, A.S. Tsao, A. S. Mansfield, S. Popat, T. Jahan, S. Antonia, Y. Oulkhouir, Y. Bautista, R. Cornelissen, L. Greillier, F. Grossi, D. Kowalski, J. Rodriguez-Cid, P. Aanur, A. Oukessou, C. Baudelet, G. Zalcman, First-line nivolumab plus ipilimumab in unresectable malignant pleural mesothelioma (CheckMate 743): a multicentre, randomised, open-label, phase 3 trial, Lancet 397 (10272) (2021) 375–386.

[4] S. Kato, B.N. Tomson, T.P. Buys, S.K. Elkin, J.L. Carter, R. Kurzrock, Genomic landscape of malignant mesotheliomas, Mol. Cancer Ther. 15 (10) (2016) 2498–2507.

[5] M. Brevet, Comparative genetics of diffuse malignant mesothelioma tumors of the peritoneumand pleura, with focus on BAP1 expression, Pleura Peritoneum 1 (2) (2016) 91–97.

[6] F. Baumann, E. Flores, A. Napolitano, S. Kanodia, E. Taioli, H. Pass, H. Yang, M. Carbone, Mesothelioma patients with germline BAP1 mutations have 7-fold improved long-term survival, Carcinogenesis 36 (1) (2015) 76–81.

[7] R. Bueno, E.W. Stawiski, L.D. Goldstein, S. Durinck, A. De Rienzo, Z. Modrusan, F. Gnad, T.T. Nguyen, B.S. Jaiswal, L.R. Chirieac, D. Sciaranghella, N. Dao, C. E. Gustafson, K.J. Munir, J.A. Hackney, A. Chaudhuri, R. Gupta, J. Guillory, K. Toy, C. Ha, Y.J. Chen, J. Stinson, S. Chaudhuri, N. Zhang, T.D. Wu, D.J. Sugarbaker, F. J. de Sauvage, W.G. Richards, S. Seshagiri, Comprehensive genomic analysis of malignant pleural mesothelioma identifies recurrent mutations, gene fusions and splicing alterations, Nat. Genet. 48 (4) (2016) 407–416.

[8] R. Noberini, R. Longuespee, C. Richichi, G. Pruneri, M. Kriegsmann, G. Pelicci, T. Bonaldi, PAT-H-MS coupled with laser microdissection to study histone post-translational modifications in selected cell populations from pathology samples, Clin. Epigenetics 9 (2017) 69.

[9] R. Noberini, D. Osti, C. Miccolo, C. Richichi, M. Lupia, G. Corleone, S.P. Hong, P. Colombo, B. Pollo, L. Fornasari, G. Pruneri, L. Magnani, U. Cavallaro, S. Chiocca, S. Minucci, G. Pelicci, T. Bonaldi, Extensive and systematic rewiring of histone post-translational modifications in cancer model systems, Nucleic Acids Res. (2018).

[10] R. Noberini, C. Restellini, E.O. Savoia, T. Bonaldi, Enrichment of histones from patient samples for mass spectrometry-based analysis of post-translational modifications, Methods (2019).

[11] R. Noberini, C. Restellini, E.O. Savoia, F. Raimondi, L. Ghiani, M.G. Jodice, G. Bertalot, G. Bonizzi, M. Capra, F.A. Maffini, M. Tagliabue, M. Ansarin, M. Lupia, M. Giordano, D. Osti, G. Pelicci, S. Chiocca, T. Bonaldi, Profiling of Epigenetic Features in Clinical Samples Reveals Novel Widespread Changes in Cancer, Cancers (Basel) 11(5) (2019).

[12] R. Noberini, A. Uggetti, G. Pruneri, S. Minucci, T. Bonaldi, Pathology tissue-quantitative mass spectrometry analysis to profile histone post-translational modification patterns in patient samples, Mol. Cell. Proteomics 15 (3) (2016) 866–877.

[13] R. Noberini, E. Longhi, T. Bonaldi, A Super-SILAC approach for profiling histone posttranslational modifications, Methods Mol. Biol. 2603 (2023) 87–102.

[14] R. Noberini, E.O. Savoia, S. Brandini, F. Greco, F. Marra, G. Bertalot, G. Pruneri, L. A. McDonnell, T. Bonaldi, Spatial epi-proteomics enabled by histone post-translational modification analysis from low-abundance clinical samples, Clin. Epigenetics 13 (1) (2021) 145.

[15] Z.F. Yuan, S. Sidoli, D.M. Marchione, J. Simithy, K.A. Janssen, M.R. Szurgot, B. A. Garcia, EpiProfile 2.0: a computational platform for processing epi-proteomics mass spectrometry data, J. Proteome Res. 17 (7) (2018) 2533–2541.

[16] S. Tyanova, T. Temu, P. Sinitcyn, A. Carlson, M.Y. Hein, T. Geiger, M. Mann, J. Cox, The Perseus computational platform for comprehensive analysis of (prote) omics data, Nat. Methods 13 (9) (2016) 731–740.

[17] J.A. Vizcaino, E.W. Deutsch, R. Wang, A. Csordas, F. Reisinger, D. Rios, J. A. Dianes, Z. Sun, T. Farrah, N. Bandeira, P.A. Binz, I. Xenarios, M. Eisenacher, G. Mayer, L. Gatto, A. Campos, R.J. Chalkley, H.J. Kraus, J.P. Albar, S. Martinez-Bartolome, R. Apweiler, G.S. Omenn, L. Martens, A.R. Jones, H. Hermjakob, ProteomeXchange provides globally coordinated proteomics data submission and dissemination, Nat. Biotechnol. 32 (3) (2014) 223–226.

[18] R. Noberini, G. Robusti, A. Vai, E.O. Savoia, M.G. Jodice, G. Bertalot, B. Cat, I. Pallavicini, G. Bonizzi, M. Capra, C.A. Sangalli, F. Zambelli, N. Fusco, S. Pece, G. Pavesi, S. Minucci, T. Bonaldi, A histone-centric multi-omics study shows that increased H3K4 methylation sustains triple-negative breast cancer phenotypes, Nat. Commun. 16 (1) (2025) 8716.

[19] M.C. Herwig-Carl, A. Sharma, V. Tischler, N. Pelusi, K.U. Loeffler, F.G. Holz, M. Zeschnigk, S. Landreville, C. Auw-Haedrich, R. Noberini, T. Bonaldi, Mass Spectrometry-based profiling of histone post-translational modifications in uveal

melanoma tissues, human melanocytes, and uveal melanoma cell lines - a pilot study, Invest. Ophthalmol. Vis. Sci. 65 (2) (2024) 27.
[20] S. Cregan, L. McDonagh, Y. Gao, M.P. Barr, K.J. O'Byrne, S.P. Finn, S. Cuffe, S. G. Gray, KAT5 (Tip60) is a potential therapeutic target in malignant pleural mesothelioma, Int. J. Oncol. 48 (3) (2016) 1290–1296.
[21] R. Noberini, D. Osti, C. Miccolo, C. Richichi, M. Lupia, G. Corleone, S.P. Hong, P. Colombo, B. Pollo, L. Fornasari, G. Pruneri, L. Magnani, U. Cavallaro, S. Chiocca, S. Minucci, G. Pelicci, T. Bonaldi, Extensive and systematic rewiring of histone post-translational modifications in cancer model systems, Nucleic Acids Res. 46 (8) (2018) 3817–3832.
[22] M. Ghizzoni, J. Wu, T. Gao, H.J. Haisma, F.J. Dekker, Y., George Zheng, 6-alkyl-salicylates are selective Tip60 inhibitors and target the acetyl-CoA binding site, Eur. J. Med. Chem. 47 (1) (2012) 337–344.
[23] J.D. Gaddameedi, T. Chou, B.S. Geller, A. Rangarajan, T.A. Swaminathan, D. Dixon, K. Long, C.J. Golder, V.A. Vuong, S. Banuelos, R. Greenhouse, M. P. Snyder, A.M. Lipchik, J.J. Gruber, Acetyl-click screening platform identifies small-molecule inhibitors of histone acetyltransferase 1 (HAT1), J. Med. Chem. 66 (8) (2023) 5774–5801.
[24] D.S. Chandrashekar, B. Bashel, S.A.H. Balasubramanya, C.J. Creighton, I. Ponce-Rodriguez, B. Chakravarthi, S. Varambally, UALCAN: a portal for facilitating tumor subgroup gene expression and survival analyses, Neoplasia 19 (8) (2017) 649–658.
[25] P. Nagarajan, Z. Ge, B. Sirbu, C. Doughty, P.A. Agudelo Garcia, M. Schlederer, A. T. Annunziato, D. Cortez, L. Kenner, M.R. Parthun, Histone acetyl transferase 1 is essential for mammalian development, genome stability, and the processing of newly synthesized histones H3 and H4, PLoS Genet. 9 (6) (2013) e1003518.
[26] E. Kettunen, H. Hernandez-Vargas, M.P. Cros, G. Durand, F. Le Calvez-Kelm, K. Stuopelyte, S. Jarmalaite, K. Salmenkivi, S. Anttila, H. Wolff, Z. Herceg, K. Husgafvel-Pursiainen, Asbestos-associated genome-wide DNA methylation changes in lung cancer, Int. J. Cancer 141 (10) (2017) 2014–2029.
[27] J. Matull, J.M. Placke, G. Lodde, A. Zaremba, J. Utikal, P. Terheyden, C. Pfohler, R. Herbst, A. Kreuter, J. Welzel, J. Kretz, I. Moller, A. Sucker, A. Paschen, E. Livingstone, L. Zimmer, E. Hadaschik, S. Ugurel, D. Schadendorf, C. M. Thielmann, K.G. Griewank, Clinical and genetic characteristics of BAP1-mutated non-uveal and uveal melanoma, Front. Immunol. 15 (2024) 1383125.
[28] P.A. Jones, S.B. Baylin, The epigenomics of cancer, Cell 128 (4) (2007) 683–692.
[29] H. Wang, K. Helin, Roles of H3K4 methylation in biology and disease, Trends Cell Biol. 35 (2) (2025) 115–128.
[30] C.J. Terranova, M. Maitituoheti, A.T. Raman, M. Tang, N.E. Anvar, A.K. Ghosh, S. B. Amin, J. Schulz, E. Orouji, F. Giancotti, P. Troncoso, C.J. Logothetis, T. Thompson, K. Rai, H3K4me1-marked Enhancer Activation in Resistant Prostate Cancers Implicates SOX4 and MENIN Inhibition as Therapeutic Strategies, bioRxiv (2021) 2021.09.02.458625.
[31] A.J. Price, M.C. Manjegowda, J. Kain, S. Anandh, I.M. Bochkis, Hdac3, Setdb1, and Kap1 mark H3K9me3/H3K14ac bivalent regions in young and aged liver, Aging Cell 19 (2) (2020) e13092.
[32] R.Z. Jurkowska, S. Qin, G. Kungulovski, W. Tempel, Y. Liu, P. Bashtrykov, J. Stiefelmaier, T.P. Jurkowski, S. Kudithipudi, S. Weirich, R. Tamas, H. Wu, L. Dombrovski, P. Loppnau, R. Reinhardt, J. Min, A. Jeltsch, H3K14ac is linked to methylation of H3K9 by the triple Tudor domain of SETDB1, Nat. Commun. 8 (1) (2017) 2057.
[33] G.K. Griffin, J. Wu, A. Iracheta-Vellve, J.C. Patti, J. Hsu, T. Davis, D. Dele-Oni, P. P. Du, A.G. Halawi, J.J. Ishizuka, S.Y. Kim, S. Klaeger, N.H. Knudsen, B.C. Miller, T. H. Nguyen, K.E. Olander, M. Papanastasiou, S. Rachimi, E.J. Robitschek, E. M. Schneider, M.D. Yeary, M.D. Zimmer, J.D. Jaffe, S.A. Carr, J.G. Doench, W. N. Haining, K.B. Yates, R.T. Manguso, B.E. Bernstein, Epigenetic silencing by SETDB1 suppresses tumour intrinsic immunogenicity, Nature 595 (7866) (2021) 309–314.
[34] J.J. Sacco, J. Kenyani, Z. Butt, R. Carter, H.Y. Chew, L.P. Cheeseman, S. Darling, M. Denny, S. Urbe, M.J. Clague, J.M. Coulson, Loss of the deubiquitylase BAP1 alters class I histone deacetylase expression and sensitivity of mesothelioma cells to HDAC inhibitors, Oncotarget 6 (15) (2015) 13757–13771.
[35] P.K. Paik, L.M. Krug, Histone deacetylase inhibitors in malignant pleural mesothelioma: preclinical rationale and clinical trials, J. Thorac. Oncol. 5 (2) (2010) 275–279.